Eur. Phys. J. C 19, 351–360 (2001)
Digital Object Identifier (DOI) 10.1007/s100520100604

THE EUROPEAN PHYSICAL JOURNAL C

Hadronic final state predictions from CCFM: the hadron-level Monte Carlo generator CASCADE*

H. Jung[1], G.P. Salam[2,3]

[1] Physics Department, Lund University, Box 118, 221 00 Lund, Sweden
[2] CERN, TH Division, Geneva, Switzerland
[3] LPTHE, Universités P. & M. Curie (Paris VI) et Denis Diderot (Paris VII), Paris, France

Received: 13 December 2000 / Published online: 15 March 2001 – © Springer-Verlag 2001

Abstract. We discuss a practical formulation of backward evolution for the CCFM small-x evolution equation and show results from its implementation in the new Monte Carlo event-generator CASCADE.

1 Introduction

In recent years a wealth of experimental results has become available from HERA concerning structure functions and final-state properties in deep inelastic collisions (DIS) at small Bjorken x and moderate Q^2 and this has led to interest in theoretical descriptions and predictions of the phenomena that are observed.

DIS at moderate values of x is well described by resummations of leading logarithms of transverse momenta $(\alpha_s \ln Q^2)^n$, generally referred to as DGLAP physics [1–4]. At small x we expect leading-logs of longitudinal momenta, $(\alpha_s \ln x)^n$, to become equally if not more important. However, while the understanding of DGLAP resummations has been mature for some time now, despite considerable effort small-x resummations still remain the subject of many theoretical uncertainties and technical difficulties.

Since many of the measurements at HERA involve complex cuts and multi-particle final states, the ideal form for any theoretical description of the data is a Monte Carlo event-generator which embodies small-x resummations, in analogy with event generators such as LEPTO [5], PYTHIA [6], HERWIG [7,8] and RAPGAP [9] which embody DGLAP resummations.

In order to build such an event generator two ingredients are required. Firstly one needs to know the underlying parton branching equation which, when iterated over many branchings, reproduces the correct leading logarithms. Secondly one has to find an efficient way of implementing the branching equation into a Monte Carlo event generator.

As it happens there are several branching equations which are advocated by various groups as suitable for describing both inclusive and exclusive properties of small-x DIS. The main purpose of this article is to discuss how to formulate one of these equations, the CCFM equation [10–13] in a manner suitable for carrying out a backward evolution. This is an almost essential requirement if one wishes to efficiently generate unweighted Monte Carlo events and modern DGLAP based Monte Carlo generators are always based on backward evolution approaches [14–16]. One of the main results of this paper is that despite the fact that the CCFM equation is considerably more complicated than the DGLAP equation, it is possible to cast the backward evolution in a form which looks quite similar to the normal DGLAP approach. We then show predictions obtained from a new Monte Carlo event generator, CASCADE, which implements the backward evolution, and compare them with HERA data.

The paper is structured as follows: in Sect. 2 we discuss briefly the reasons for choosing the CCFM equation for the underlying branching. Then in Sect. 3 we discuss the CCFM equation itself, and review some details of its implementation in the forward-evolution Monte Carlo event-generator SMALLX [17,18], which has been used to generate the unintegrated gluon distribution required by the backward evolution. In Sect. 4 we discuss the backward evolution itself, and then in Sect. 5 show some results.

2 Why CCFM?

There are three equations which are commonly used for predictions in small-x DIS: the BFKL equation [19–21], the CCFM equation [10–13] and the LDC equation [22–25].

The BFKL and CCFM approaches are known to reproduce the correct small-x leading logarithms for the total cross section. For final-state properties, the derivation of the BFKL equation is such that it is not able to guarantee the correctness of the small-x logarithms. On the other hand the derivation of the CCFM equation, based on the principle of colour coherence, is such that it guarantees

* Research supported in part by E.U. QCDNET contract FMRX-CT98-0194

the correct leading logarithms for all final-state observables. (It so happens that the CCFM equation also gives a correct description of the final state in the limit $x \to 1$, another region particularly sensitive to coherence effects, however this is not relevant for our purposes).

This was the situation until a couple of years ago. Recently however it was shown that BFKL gives identical leading logarithms of x to CCFM for all final-state observables [26–28] (the physical reasons for this are not fully understood). Since the BFKL equation is quite simple (compared to CCFM) one might think that this opens the way to a BFKL-based Monte Carlo for DIS. But from the point of view of a *sensible* description of exclusive quantities, it is not just the leading logarithms which matter. For example with the current state of the art, one has two options when implementing the BFKL equation in a event generator for DIS. One possibility is to use x as the evolution variable — but it turns out that for some observables this introduces a weak (but pathological) dependence on one's infrared cutoff in the subleading logarithms of x, $\alpha_s^p(\alpha_s \ln x)^n$ $(p > 0)$ [28]. The second way of implementing BFKL, which resolves this problem, is to use rapidity as the evolution variable. But this turns out to be at the expense of introducing subleading logarithms $(\alpha_s \ln^2 Q^2)^n$ which violate renormalisation group considerations[1]. Specifically DGLAP, CCFM and BFKL with x as the evolution variable all predict that F_2 at small x and large Q^2 should behave as

$$F_2(x, Q^2) \sim \exp\left(2\sqrt{\bar{\alpha}_s \ln Q \ln 1/x}\right)$$

(where $\bar{\alpha}_s = \alpha_s C_A/\pi$ and we use fixed α_s for the purposes of illustration). For BFKL with rapidity as the evolution variable one has to substitute $\ln 1/x$ with the rapidity difference between the two ends of the chain $\Delta\eta \simeq \ln Q/x$, and this leads to F_2 behaving as

$$F_2(x, Q^2) \sim \exp\left(2\sqrt{\bar{\alpha}_s \ln Q \ln 1/x + \bar{\alpha}_s \ln^2 Q}\right),$$

in contradiction to the DGLAP result.

The CCFM equation does not suffer from these problems and so forms a good basis for an event generator. This does not mean that the CCFM equation embodies all of our knowledge about small-x branching, in particular it is known to be incomplete in regions of phase space where there is collinear or anti-collinear branching. Furthermore it was discovered in [32] that seemingly small modifications of the equation can lead to big differences in its predictions. Specifically in a version of the equation without the $1/(1-z)$ part of the splitting function, the replacement of $\Theta(k_t - q)$ with $\Theta(k_t - (1-z)q)$ in the non-Sudakov form factor, (12), was instrumental in enabling a fit to F_2. However around the same time the exact next-to-leading logarithmic (NLL) corrections to small-x evolution, terms $\alpha_s(\alpha_s \ln x)^n$, became available [33,34]: they state that the power ω governing the growth of quantities like the forward-jet cross section at small x should have an expansion $\omega = 4 \ln 2\bar{\alpha}_s - 18.4\bar{\alpha}_s^2 + \ldots$ (for $n_f = 4$). On the other hand the version of the CCFM equation with the replacement $\Theta(k_t - q) \to \Theta(k_t - (1-z)q)$ in the non-Sudakov form factor leads to $\omega = 4 \ln 2\bar{\alpha}_s - (75 \pm 4)\bar{\alpha}_s^2 + \ldots$, which is quite incompatible with the known expansion [33,34] and so this variant of the CCFM equation can be ruled out. The version of the CCFM equation that is studied here has $\omega = 4 \ln 2\bar{\alpha}_s - (9.2 \pm 0.5)\bar{\alpha}_s^2 + \ldots$ [35] — i.e. its NLL corrections are somewhat smaller than the true NLL corrections, however they are at least of the right order of magnitude.

There exists also a third evolution equation, the Linked Dipole Chain (LDC) [22–25], whose characteristic is that some of the initial state radiation has been moved into the final state. This has two consequences — on one hand the simplifications that ensue mean that it is quite easy to correctly implement a symmetry between branching up and down in transverse scale (or equivalently one obtains the same predictions whether one evolves from the virtual photon or from the proton). Such a symmetry leads to the implicit inclusion of important NLL terms associated with large transverse logs in the anti-collinear limit (terms $\bar{\alpha}_s^2/(1-\gamma)^3$ where γ is the Mellin variable conjugate to squared transverse momentum). These terms are entirely missing from standard LL BFKL, while in CCFM they are present, but with half the correct coefficient[2]. The second consequence of the manner in which initial state radiation has been moved into the final state, is that the LDC has slightly different small-x leading logs compared to BFKL ($\omega \simeq 3.23\bar{\alpha}_s + \ldots$ for LDC as compared to $\omega \simeq 2.77\bar{\alpha}_s + \ldots$ for BFKL and CCFM — it is possible though to modify LDC so that it has leading logs which are much closer to the BFKL ones [37]). Therefore LDC has both advantages and disadvantages compared to CCFM. The question of which matters more will almost certainly depend on the nature of the observable under study.

So there remains much room for further theoretical progress in the description of small-x evolution. However given the current situation, one of the more viable options is the CCFM equation, hence our interest in implementing a practical CCFM-based event generator.

3 The CCFM evolution equation

The implementation of CCFM [10–13] parton evolution in the forward evolution Monte Carlo program SMALLX is described in detail in [17,18]. Here we only concentrate on the basic ideas and discuss the new treatment of the non-Sudakov form factor [38,39].

Figure 1 shows the pattern of QCD initial-state radiation in a small-x DIS event, together with labels for the

[1] For certain restricted applications in hadron-hadron scattering, where BFKL generators have been advocated and developed [29–31], these double-logarithms may not be too important because of the nature of the observables studied

[2] There have been attempts to implement the so-called kinematic constraint [10,22,36], which in BFKL does lead to the correct NLL behaviour for $\gamma \to 1$. But in CCFM the situation is more subtle and a straightforward inclusion of the kinematic constraint still gives the wrong $\gamma \to 1$ limit

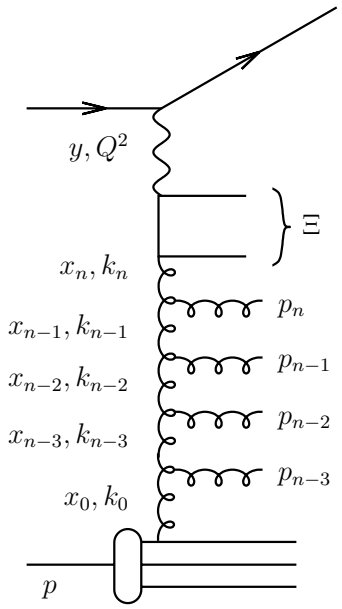

Fig. 1. Kinematic variables for multi-gluon emission. The t-channel gluon four-vectors are given by k_i and the gluons emitted in the initial state cascade have four-vectors p_i. The upper angle for any emission is obtained from the quark box, as indicated with Ξ

kinematics. According to the CCFM evolution equation, the emission of partons during the initial cascade is only allowed in an angular-ordered region of phase space. The maximum allowed angle Ξ is defined by the hard scattering quark box[3], which connects the gluon to the virtual photon. In terms of Sudakov variables the quark pair momentum is written as:

$$p_q + p_{\bar{q}} = Y(p_p + \Xi p_e) + Q_t \tag{1}$$

where p_p and p_e are the proton and electron momenta, respectively and Q_t is the transverse momentum of the quark pair. Similarly, the momenta p_i of the gluons emitted during the initial state cascade are given by (here treated massless):

$$p_i = y_i(p_p + \xi_i p_e) + p_{ti}\ , \quad \xi_i = \frac{p_{ti}^2}{s y_i^2}, \tag{2}$$

with $y_i = (1 - z_i)x_{i-1}$ and $x_i = z_i x_{i-1}$ and $s = (p_p + p_e)^2$ being the total electron proton center of mass energy. The variable ξ_i is connected to the angle of the emitted gluon with respect to the incoming proton and x_i and y_i are the momentum fractions of the exchanged and emitted gluons, while z_i is the momentum fraction in the branching $(i-1) \to i$ and p_{ti} is the transverse momentum of the emitted gluon.

The angular-ordered region is then specified by:

$$\xi_0 < \xi_1 < \cdots < \xi_n < \Xi \tag{3}$$

which becomes:

$$z_{i-1} q_{ti-1} < q_{ti} \tag{4}$$

where we use the rescaled transverse momenta q_{ti} of the emitted gluons defined by:

$$q_{ti} = x_{i-1}\sqrt{s\xi_i} = \frac{p_{ti}}{1 - z_i}\ . \tag{5}$$

In SMALLX, the initial state gluon cascade is generated in a forward evolution approach from an initial distribution of the k_t unintegrated gluon distribution according to:

$$x\mathcal{A}_0(x, k_{t0}^2) = N \cdot 5 \frac{1}{k_0^2}(1 - x)^4 \cdot \exp\left(-k_{t0}^2/k_0^2\right) \tag{6}$$

where N is a normalization constant. The exponential distribution in k_t^2 has a width which will be set to $k_0^2 = 1\ \mathrm{GeV}^2$. The input gluon distribution needs to be adjusted to fit existing data, but it turns out that the small x behaviour of the structure function F_2 is rather insensitive to the actual choice of $x\mathcal{A}_0(x, k_{t0}^2)$ and only the normalization N acts as a free parameter, with the constraint:

$$\int x\mathcal{A}_0(x, k_{t0}^2) dx dk_{t0}^2 = \int x G_0(x, Q^2) dx \simeq 0.5 \tag{7}$$

which gives:

$$\int x\mathcal{A}_0(x, k_{t0}^2) dx dk_{t0}^2 = N \cdot 5 \cdot \int (1 - x)^4 dx = N\ . \tag{8}$$

The initial state branching of a gluon k_i into another virtual (t-channel) gluon k_{i+1} and a final gluon p_{i+1} (treated on mass shell) is generated iteratively from the initial gluon distribution at a starting scale Q_0. The probability for successive branchings to occur is given by the CCFM splitting function [10–13]:

$$dP_i = \tilde{P}_g^i(z_i, q_i^2, k_{ti}^2) \cdot \Delta_s dz_i \frac{d^2 q_i}{\pi q_i^2} \cdot \Theta(q_i - z_i q_{i-1}) \cdot \Theta(1 - z_i - \epsilon_i) \tag{9}$$

with $q_i = p_{ti}/(1 - z_i)$ being the rescaled transverse momentum of the emitted gluon i. The fractional energy of the exchanged gluon i is given by x_i and the energy transfer between the exchanged gluons $i - 1$ and i is given by $z_i = x_i/x_{i-1}$. A collinear cutoff $\epsilon_i = Q_0/q_i$ is introduced to regularize the $1/(1 - z)$ singularity. The Sudakov form factor Δ_s is given by:

$$\Delta_s(q_i, z_i q_{i-1}) = \exp\left(-\int_{(z_{i-1}q_{i-1})^2}^{q_i^2} \frac{dq^2}{q^2} \int_0^{1 - Q_0/q} dz \times \frac{\bar{\alpha}_s(q^2(1 - z)^2)}{1 - z}\right) \tag{10}$$

with $\bar{\alpha}_s = \frac{C_A \alpha_s}{\pi} = \frac{3\alpha_s}{\pi}$. For inclusive quantities at leading-logarithmic order the Sudakov form factor cancels against the $1/(1 - z)$ collinear singularity of the splitting function. Coherence effects are taken into account by angular ordering $q_i > z_{i-1} q_{i-1}$ given by the first Θ function in (9).

[3] Strictly there are two maximum angles, corresponding to the directions of the quark and the anti-quark, and which each limit roughly one half of the radiation

The cascade continues until q_i reaches the limiting angle defined by $\bar{q} = x_n\sqrt{s\Xi}$, set by the partons from the hard scattering matrix element.

The gluon splitting function $\tilde{P}_g^i$ is given by[4]:

$$\tilde{P}_g^i = \frac{\bar{\alpha}_s(q_i^2(1-z_i)^2)}{1-z_i} + \frac{\bar{\alpha}_s(k_{ti}^2)}{z_i}\Delta_{ns}(z_i, q_i^2, k_{ti}^2) \qquad (11)$$

where the non-Sudakov form factor Δ_{ns} is defined as:

$$\log\Delta_{ns} = -\bar{\alpha}_s(k_{ti}^2)\int_0^1 \frac{dz'}{z'}\int\frac{dq^2}{q^2}\Theta(k_{ti}-q)\Theta(q-z'q_{ti})\,. \qquad (12)$$

The principal difference compared to the corresponding DGLAP splitting function is the appearance of the non-Sudakov form factor Δ_{ns}, which screens the $1/z$ singularity in (11). It can be expressed as [36]:

$$\log\Delta_{ns} = -\bar{\alpha}_s(k_{ti}^2)\log\left(\frac{z_0}{z_i}\right)\log\left(\frac{k_{ti}^2}{z_0 z_i q_i^2}\right) \qquad (13)$$

where

$$z_0 = \begin{cases} 1 & \text{if} k_{ti}/q_i > 1 \\ k_{ti}/q_i & \text{if} z_i < k_{ti}/q_i \le 1 \\ z_i & \text{if} k_{ti}/q_i \le z_i \end{cases}$$

which means that in the region $k_{ti}/q_i \le z_i$ we have $\Delta_{ns} = 1$, giving no suppression at all[5].

The CCFM equation for the unintegrated gluon density can be written [13,32,36] as an integral equation:

$$\mathcal{A}(x,k_t,\bar{q}) = \mathcal{A}_0(x,k_t,\bar{q}) + \int\frac{dz}{z}\int\frac{d^2q}{\pi q^2}\Theta(\bar{q}-zq) \times\Delta_s(\bar{q},zq)\tilde{P}(z,q,k_t)\mathcal{A}\left(\frac{x}{z},k_t',q\right) \qquad (14)$$

with $k_t' = |\mathbf{k}_t + (1-z)\mathbf{q}|$ and with $\bar{q}$ being the upper scale for the last angle of the emission: $\bar{q} > z_n q_n$, $q_n > z_{n-1}q_{n-1}$,..., $q_1 > Q_0$. As before q is used as a shorthand notation for the 2-dimensional vector of the rescaled transverse momentum $\mathbf{q} \equiv \mathbf{q}_t = \mathbf{p}_t/(1-z)$. The splitting function $\tilde{P}(z,q,k_t)$ is defined in (11) and the Sudakov form factor $\Delta_s(\bar{q},zq)$ is given in (10).

In [13] a differential form of the CCFM evolution equation is given, which is obtained from (14) by dividing both sides by $\Delta_s(\bar{q},Q_0)$ and then differentiating with respect to $\bar{q}$:

$$\bar{q}^2\frac{d}{d\bar{q}^2}\frac{x\mathcal{A}(x,k_t,\bar{q})}{\Delta_s(\bar{q},Q_0)} = \int dz\frac{d\phi}{2\pi}\frac{\tilde{P}(z,\bar{q}/z,k_t)}{\Delta_s(\bar{q},Q_0)}\,x'\mathcal{A}(x',k_t',\bar{q}/z) \qquad (15)$$

with $x' = x/z$ and $k_t' = |(1-z)/z\mathbf{q} + \mathbf{k_t}|$ and where $\mathbf{q}$ has an azimuthal angle ϕ. In deriving this equation we have exploited the fact that the Sudakov form factor can be written as

$$\Delta_s(\bar{q},zq) = \frac{\Delta_s(\bar{q},Q_0)}{\Delta_s(zq,Q_0)}\,. \qquad (16)$$

For (15) (and the backward evolution formalism which follows from it) to be correct $\mathcal{A}_0(x,k_t,\bar{q})$, must be of the form

$$\mathcal{A}_0(x,k_t,\bar{q}) = \mathcal{A}_0(x,k_t)\,\Delta_s(\bar{q},Q_0)\,. \qquad (17)$$

4 Backward evolution: CCFM and CASCADE

The forward evolution procedure as implemented in SMALLX is a direct way of solving the CCFM evolution equation including the correct treatment of the kinematics in each branching. However the forward evolution is rather time consuming, since in each branching a weight factor is associated, and only after the initial state cascade has been generated completely can it be decided whether the kinematics allow the generation of the hard scattering process. Quite often, a complete event has to be rejected.

A more efficient procedure to adopt in a full hadron-level Monte Carlo generator is a backward evolution scheme, analogous to that used in standard Monte Carlo programs [15,14,7] using a DGLAP type parton cascade. The idea is to first generate the hard scattering process with the initial parton momenta distributed according to the parton distribution functions. This involves in general only a fixed number of degrees of freedom, and the hard scattering process can be generated quite efficiently. Then, the initial state cascade is generated by going backwards from the hard scattering process towards the beam particles. In a DGLAP type cascade the evolution (ordering) is done usually in the virtualities of the exchanged t-channel partons.

According to the CCFM equation the probability of finding a gluon in the proton depends on three variables, the momentum fraction x, the transverse momentum squared k_t^2 of the exchanged gluons and the maximum angle allowed for any emission $\bar{q} = x_n\sqrt{s\Xi}$. To calculate this probability, in addition to the details of the splitting, (9) one needs to know the unintegrated gluon distribution $\mathcal{A}(x,k,\bar{q})$ which has to be determined beforehand.

Given this distribution, the generation of a full hadronic event has three steps, implemented in a new hadron-level Monte Carlo program, CASCADE:

- Firstly, the hard scattering process is generated,

$$\sigma = \int dk_t^2 dx_g \mathcal{A}(x_g,k_t^2,\bar{q})\sigma(\gamma^* g^* \to q\bar{q})\,, \qquad (18)$$

using the off-shell matrix elements given in [40, p. 178 ff], with the gluon momentum (in Sudakov representation):

$$k = x_g p_p + \bar{x}_g p_e + k_t \simeq x_g p_p + k_t\,. \qquad (19)$$

The gluon virtuality is then $-k^2 \simeq k_t^2$.

[4] Actually the 'correct' scale for α_s, as suggested by the NLL corrections to BFKL, is probably $q_i^2(1-z_i)^2$ in both terms, with a corresponding modification of the non-Sudakov form factor. However for simplicity, at this stage we have retained the scale for α_s that was present in the original formulation of SMALLX

[5] We note that in the original version of SMALLX a simplified version of the non-Sudakov form factor was used, which however did not give the right answer for $k_t < q$

- The initial state cascade is generated according to CCFM in a backward evolution approach (described in the next section).
- The hadronisation is performed using the Lund string fragmentation implemented in JETSET [41].

Strictly speaking, before the last step one should also include angular-ordered final-state radiation from the initial state gluons. For simplicity, in this 'proof of concept' version of the generator, this is currently left out.

In the backward evolution there is one difficulty: The gluon virtuality enters in the hard scattering process and also influences the kinematics of the produced quarks and therefore the maximum angle allowed for any further emission in the initial state cascade. This virtuality is only known after the whole cascade has been generated, since it depends on the history of the gluon evolution. In the evolution equations itself it does not enter, since there only the longitudinal energy fractions z_i and the transverse momenta are involved. This problem can only approximately be overcome by using $k^2 = k_t^2/(1-x_g)$ for the virtuality which is correct in the case of no further gluon emission in the initial state.

The Monte Carlo program CASCADE can be used to generate unweighted full hadron-level events, including initial-state parton evolution according to the CCFM equation and the off-shell matrix elements for the hard scattering process. It is suitable both for photo-production of heavy quarks as well as for deep inelastic scattering. The typical time needed to generate one event is ~ 0.03 sec, which is similar to the time needed by standard Monte Carlo event generators such as LEPTO [5] or PYTHIA [6].

4.1 The unintegrated gluon density

The unintegrated gluon density $x\mathcal{A}(x,k_t^2,\bar{q})$ is obtained from a forward evolution procedure as implemented in SMALLX[17,18]. Due to the complicated structure of the CCFM equation, no attempt is made to parameterize the unintegrated gluon density. Instead, the gluon density is calculated on a grid in $\log x$, $\log k_t$ and $\log \bar{q}$ of $50\times 50\times 50$ points and then linear interpolation is used to obtain the gluon density at values in between the grid points.

From the initial gluon distribution as used in SMALLX (including the same collinear cutoff and normalization) a set of values $x_{0\,i}$ and $k_{t0\,i}$ are obtained by evolving up to a given scale $\log \bar{q}$ using the forward evolution procedure of SMALLX. This is repeated 10^7 times thus obtaining a distribution of the unintegrated gluon density $x_n\mathcal{A}(x_n,k_{t\,n}^2,q_{t\,n})$ for the slice of phase space with a given $\bar{q}$ ($\bar{q} > q_{t\,n}$). To obtain a distribution in $\log \bar{q}$, the above procedure is repeated from the beginning 50 times for the different grid points in $\log \bar{q}$ up to $\bar{q} = 1800$ GeV.

4.2 Backward evolution formalism

In the backward evolution we start from the quark box, with an upper angle given by Ξ and a gluon four-vector k_n (see Fig. 1) and go successively down in the ladder until we end up at gluon k_0. Thus the first step is to reconstruct from Ξ and k_n the vectors $q_n = p_n/(1-z_n)$ and $k_{n-1} = k_i$, with $z_n = x_i/x_n$. In the next step k_i, q_n play the role of k_n, Ξ from the first step. In the further steps k_{i-1}, q_i play the role of k_i, q_{i+1} and so on, until the gluon k_0 is reached.

The differential form of the evolution equation (15) gives the (non-normalized) probability [15], that during a small decrease of $\bar{q}$, a t-channel gluon k' with momentum fraction x' becomes resolved into a t-channel gluon k with momentum fraction $x = zx'$ and an emitted gluon q_i. During a small decrease of $\bar{q}$, a gluon k may be unresolved into a gluon k'. The normalized probability for this to happen is given by

$$\frac{\Delta_s(\bar{q},Q_0)}{x\mathcal{A}(x,k_t,\bar{q})}\, d\left(\frac{x\mathcal{A}(x,k_t,\bar{q})}{\Delta_s(\bar{q},Q_0)}\right) = \frac{d\bar{q}^2}{\bar{q}^2}\int dz \frac{d\phi}{2\pi}\,\tilde{P}(z,\bar{q}/z,k_t)\frac{x'\mathcal{A}(x',k_t',\bar{q}/z)}{x\mathcal{A}(x,k_t,\bar{q})}\,. \quad (20)$$

This equation can be integrated between $\bar{q}$ and q giving:

$$\log\left(\frac{\mathcal{A}(x,k_t,q)}{\mathcal{A}(x,k_t,\bar{q})}\frac{\Delta_s(\bar{q},Q_0)}{\Delta_s(q,Q_0)}\right) = -\int_q^{\bar{q}}\frac{dq'^2}{q'^2}\int dz\frac{d\phi}{2\pi}\,\tilde{P}(z,q'/z,k_t)\frac{x'\mathcal{A}(x',k_t',q'/z)}{x\mathcal{A}(x,k_t,q')} \quad (21)$$

Thus the probability for no radiation in the angular ordered region between $\bar{q}$ and q is just given by a new effective form factor for the backward evolution:

$$\mathcal{P}_{no\ rad}(\bar{q},q) = \exp\left(-\int_q^{\bar{q}}\frac{dq'^2}{q'^2}\int dz\frac{d\phi}{2\pi}\,\tilde{P}(z,q'/z,k_t) \times\frac{x'\mathcal{A}(x',k_t',q'/z)}{x\mathcal{A}(x,k_t,q')}\right). \quad (22)$$

In principle one could equally well just use

$$\mathcal{P}_{no\ rad}(\bar{q},q) = \frac{\mathcal{A}(x,k_t,q)}{\mathcal{A}(x,k_t,\bar{q})}\frac{\Delta_s(\bar{q},Q_0)}{\Delta_s(q,Q_0)}\,, \quad (23)$$

which is more akin to the backward evolution approach of [16]. One can see that this is the correct probability since from (14) it corresponds to the fraction of $\mathcal{A}(x,k_t,\bar{q})$ which comes from angles below q. Though (22) looks more complicated than (23), it turns out that the former is numerically more suited to our particular situation, because it is less sensitive to imprecisions and irregularities of $\mathcal{A}(x,k,q)$ (which we recall is generated by a forward evolution Monte Carlo approach). The standard DGLAP backward evolution equation would be obtained from (20) by setting $\Delta_{ns} = 1$ in the splitting function $\tilde{P}$ and replacing the argument $\bar{q}/z$ in the parton density function in the r.h.s. of (20) with $\bar{q}$.

In the CCFM backward evolution, starting with the gluon k_n, we need to reconstruct the momentum of the next emitted gluon q_n as well as that of the next exchanged gluon, k_{n-1}. This is done as follows. We start with $\bar{q} = \Xi$. Then

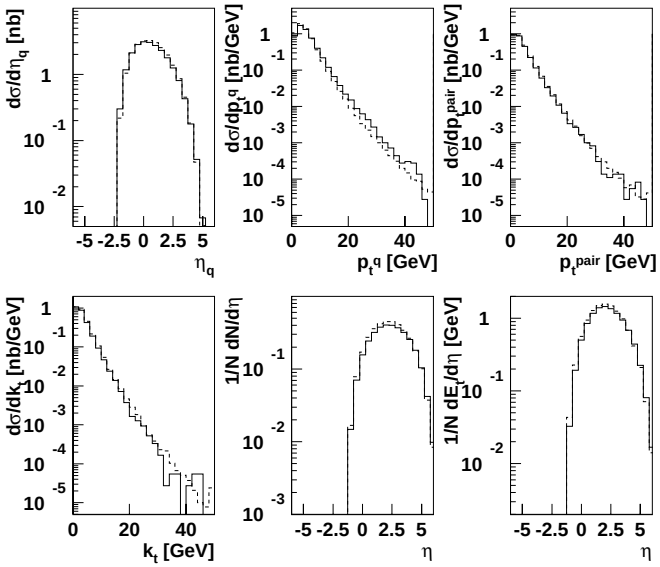

Fig. 2. Comparison of the cross section obtained from the backward evolution Monte Carlo CASCADE (solid line) with SMALLX (dashed line) both at parton level only. The upper plots show the cross section as a function of the quark rapidity η_q, the quark transverse momentum p_t and the transverse momentum of the quark pair p_t^{pair}. The lower plots show the cross section as a function of the gluon transverse momentum k_t, and the multiplicity and transverse energy flow of the gluons from the initial state cascade as a function of the rapidity η

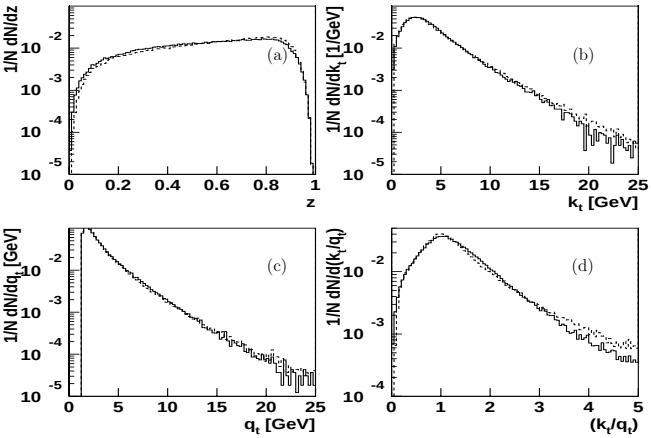

Fig. 3a–d. Comparison of quantities of the initial cascade obtained from the backward evolution Monte Carlo CASCADE (solid line) with SMALLX (dashed line) both at parton level only; **a** shows the splitting variable z, **b** gives the transverse momentum k_t, **c** shows the transverse momentum of the emitted gluon q_t, and **d** shows the ratio k_t/q_t

a. We check whether there is any evolution to be done. The probability that the evolution should stop straight away is given by

$$\frac{\mathcal{A}_0(x_n, k_{tn}^2, \bar{q})}{\mathcal{A}(x_n, k_{tn}^2, \bar{q})}\,, \tag{24}$$

i.e. the fraction of the unintegrated gluon distribution that comes from the initial distribution.

b. If the evolution continues then the quantity $q' \equiv |z_n q_n|$ is determined by choosing a random number R uniformally distributed between 0 and 1 and solving $\mathcal{P}_{no\,rad}\,(\bar{q}, q') = R$ for q'.

c. The values of z_n and ϕ_n are then chosen randomly according to the distribution given in the inner integral of (22). In doing so we implicitly have to reconstruct k_{n-1} as well.

This completes the reconstruction of a single branching. The procedure is then repeated with $\bar{q} = q_n$ and $n \to n-1$, and so on, until the evolution stops (step *a*).

In practice the numerical calculation of the integrals in the effective form factor (22) would be too time consuming, since they involve the non-Sudakov form factor in the splitting function and also the ratio of the structure functions. A simple solution to the problem is the veto algorithm described in [15]. The essential point is to find a simple analytically integrable function, which is always larger than the integrand in (22). The splitting function $\tilde{P}(z, q', k_t)$ can be replaced with:

$$P_{gg}^{appr}(z_i, k_{ti}^2) = \frac{\bar{\alpha}_s(k_{ti})}{z_i} + \frac{\bar{\alpha}_s(q_{t\,min})}{1 - z_i} \geq \tilde{P}_{gg}\,. \tag{25}$$

The limits on z_i are given by:

$$x_i \leq z_i \leq 1 - \frac{x_i Q_0}{q_{i+1}},$$

which is a larger range than the true one: $z_i < 1 - Q_0/q_i$ (but q_i is not determined at this stage). Next, the structure functions which appear in the Sudakov form factor are replaced with their maximum and minimum values for x and $x' > x$. Thus a simple analytically calculable form of the Sudakov form factor is obtained:

$$\mathcal{P}_{no\,rad}^{simple} = \exp\left(-\int_q^{\bar{q}} \frac{dq'^2}{q'^2} \int dz P_{gg}^{appr}(z, k_t) \times \frac{x' \mathcal{A}_{max}(x > x')}{x \mathcal{A}_{min}(x, k_t)}\right) < \mathcal{P}_{no\,rad}\,. \tag{26}$$

After q_i and z_i is generated, the true limits on z can be applied: $x_i \leq z_i < 1 - Q_0/q_i$. If a z_i lies outside the true region, a new set of q_i and z_i is generated. Having generated the branching variables according to z_i, k_{ti-1} and q_i according to (26) and (25), a branching is accepted with a probability according to the ratio of the integrands of $\mathcal{P}$ (via (22)) and $\mathcal{P}_{no\,rad}^{simple}$ (via (26)), as formulated in the veto algorithm [15].

As mentioned already above, the true virtuality of the t-channel gluons can only be reconstructed after the full cascade has been generated. By going from the last gluon (closest to the proton), which has virtuality $k_0^2 = k_{t0}/(1 - x_0)$, forward in the cascade to the hard scattering process, the true virtualities of the k_i^2 are reconstructed. At the end, the gluon entering to the quark box will have a larger virtuality than without initial state cascade. Thus a check is performed as to whether the production of the quarks

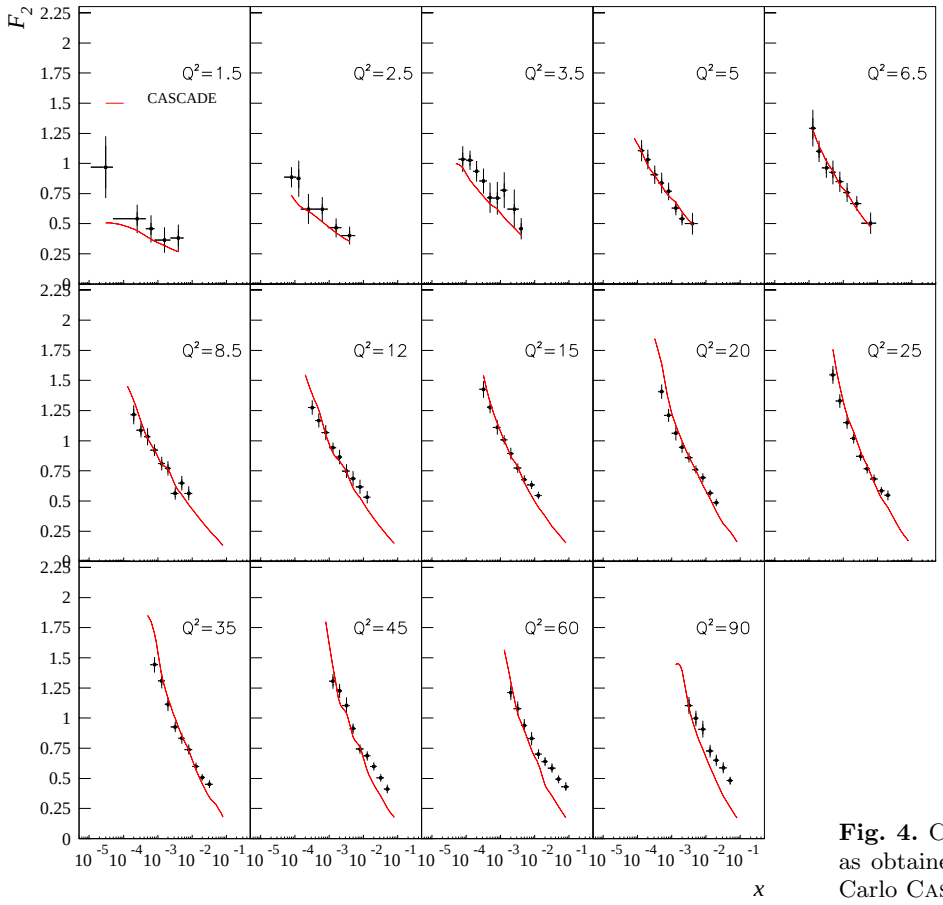

Fig. 4. Comparison of the structure function F_2 as obtained from the backward evolution Monte Carlo CASCADE with H1 data [42]

is still kinematically allowed. If not, the whole cascade is rejected, and the event without the cascade is kept. This typically happens about 1% of the time.

4.3 Comparison with the forward evolution cascade in SMALLX

In this section, the reconstruction of the parton level cascade obtained in the backward evolution approach, as described above, is compared to that of the forward evolution in SMALLX. At parton level, both approaches are expected to be identical, but small differences can occur due to the finite grid size used to define of the unintegrated gluon density. As already mentioned the virtuality of the gluon entering the hard scattering process is only known after the complete reconstruction of the initial state cascade, which could also result in small differences to the forward evolution approach. In the following comparison, we have used $b\bar{b}$ photoproduction at $\sqrt{s} = 300$ GeV. In Fig. 2 the cross section as a function of the rapidity (all rapidities are given in the laboratory frame) of the quarks η_q, the quark transverse momentum p_t^q, the transverse momentum of the quark pair p_t^{pair} and the gluon transverse momentum k_t obtained from CASCADE (solid line) are compared to the ones obtained from SMALLX (dashed line). The quantities related to the hard scattering matrix element agree very well. Also shown in Fig. 2 is a comparison of the multiplicity and the transverse energy flow as a function of rapidity, and perfect agreement is again found between the backward and forward evolution approaches. In Fig. 3 a more detailed comparison of the kinematics in the initial state cascade is performed. We compare the values of the splitting variable z, the transverse momenta k_t and q_t as well as k_t/q_t within the two approaches.

Thus we have described a backward evolution approach, which is fast and already implemented in the hadron-level Monte Carlo program CASCADE, and which reproduces perfectly the parton level configurations obtained from SMALLX. This is the first time that a practical CCFM-based small-x Monte Carlo event generator has been constructed.

5 Results

In this section we compare predictions from CASCADE with recent measurements made at HERA. The free parameters of the initial gluon distribution were fitted to describe the structure function $F_2(x, Q^2)$ in the range $x < 10^{-2}$ and $Q^2 > 5$ GeV^2. The structure function $F_2(x, Q^2)$ as calculated from CASCADE is compared to a larger range of data in Fig. 4. Reasonable agreement with the data is observed at small x and Q^2. Deviations from the data are seen at larger x and Q^2, which can be attributed to the quark contributions, which are still missing here.

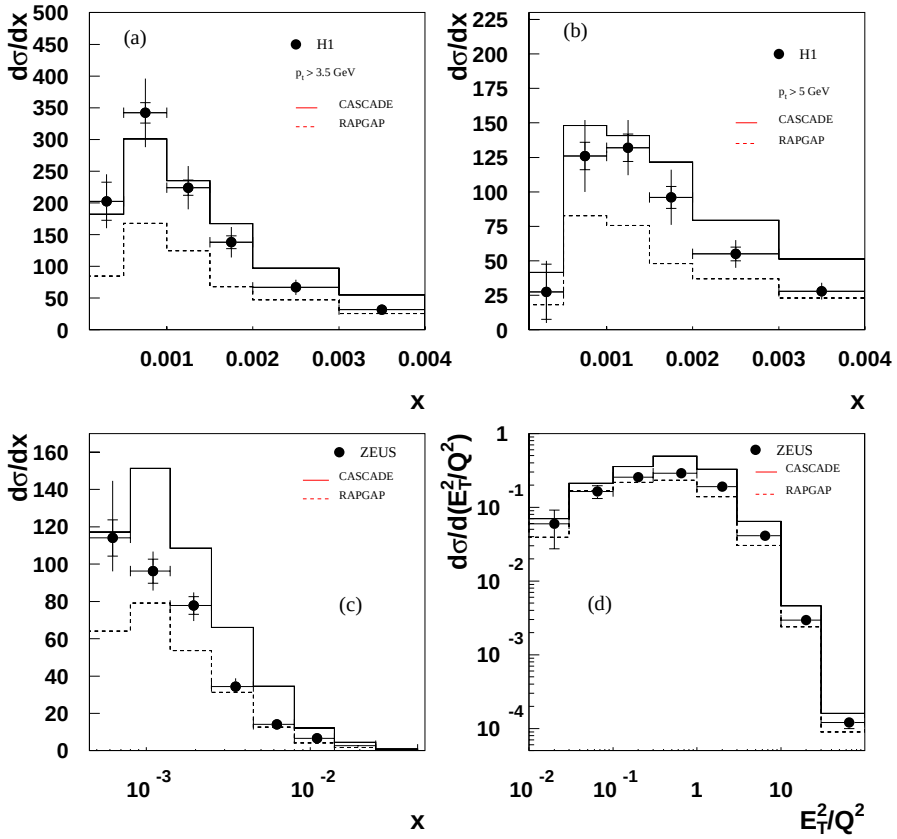

Fig. 5a–d. The cross section for forward-jet production obtained from the Monte Carlo Cascade at hadron level (solid line); **a**–**c** The cross section for forward-jet production as a function of x, for different cuts in p_t compared to H1 data [43] **a**–**b** and compared to ZEUS data [44] **c**; **d** The cross section for forward-jet production as a function of E_T^2/Q^2 compared to [45]

In Fig. 5 the cross section predicted for forward-jet production is shown and compared to measurements done at HERA. We observe a reasonable description of the data. However, the prediction lies above the data, which could indicate that some relevant sub-leading effects are still missing.

Studies based on a variety of QCD-based Monte Carlos have demonstrated that the high p_T tail of charged particle transverse momentum spectra is sensitive to small x dynamics of the parton radiation and that there is relatively little dependence on the particular model of hadronisation that is used [46,47]. Fig. 6 shows the p_T distributions of charged particles as measured by H1 [48] for DIS events with 3 GeV$^2 < Q^2 < 70$ GeV^2 in the rapidity range $0.5 < \eta < 1.5$. The prediction from Cascade gives a good description of the data, whereas DGLAP based Monte Carlo calculations fail to describe the data at small x and large p_t.

Effects of small x parton dynamics could also show up in photo-production of charm mesons. Recent measurements [49] show significant deviations from LO and NLO QCD calculations and also from hadron-level Monte Carlo predictions. In Fig. 7*a* we show the cross section of D^* production as a function of the transverse momentum $p_t^{D^*}$ using Cascade and compare it with the measurement of ZEUS [49]. For comparison we also show the prediction from Rapgap. In Fig. 7*b* the x_γ cross section is shown. In Fig. 8 we show the D^* cross section as a function of the pseudo-rapidity η^{D^*} for different regions in p_t. In all distributions of D^* photo-production we observe a

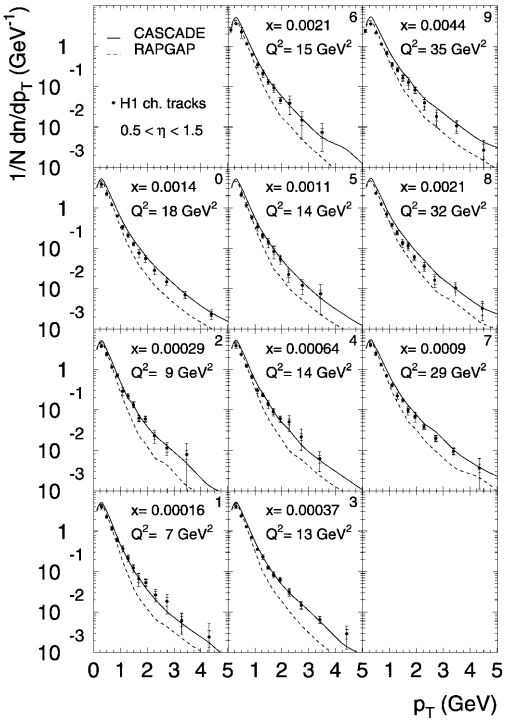

Fig. 6. The transverse momentum distribution of particles in different bins of rapidity. The prediction from Cascade (solid line) at hadron level is compared to the measurement of H1 [48]. For comparison the prediction from the DGLAP based Monte Carlo Rapgap (dashed line) is also shown

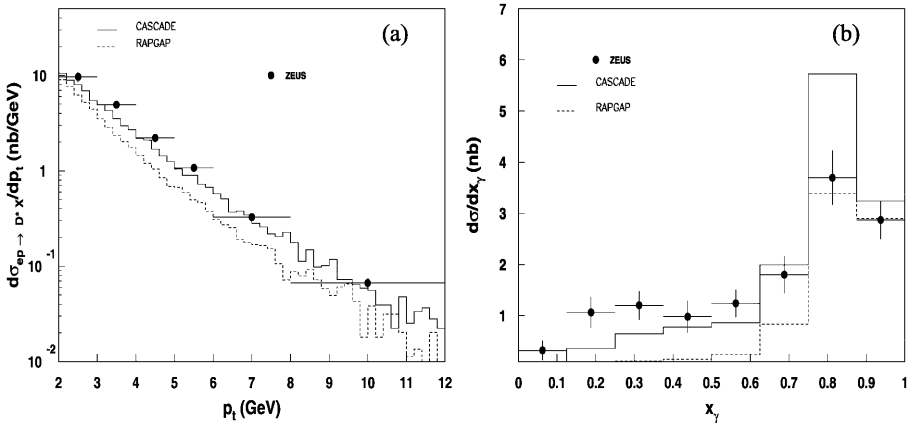

Fig. 7a,b. The differential cross sections of D^* photo-production [49] for $d\sigma/dp_t^{D^*}$ (a) and $d\sigma/dx_\gamma$ (b). The solid line shows the prediction from CASCADE while the dashed line shows the prediction from RAPGAP

good description of the experimental data, whereas there is disagreement between the data and the RAPGAP Monte Carlo predictions.

Also interesting is the cross section for $b\bar{b}$ production as measured at HERA by H1 [50]:

$$\sigma(ep \to e' b\bar{b} X) = 7.1 \pm 0.6(stat.)^{+1.5}_{-1.3}(syst.) \text{ nb}$$

to be compared with the prediction from CASCADE:

$$\sigma(ep \to e' b\bar{b} X) = 5.2^{+1.1}_{-0.9} \text{ nb}.$$

The central value is given for $m_b = 4.75$ GeV, and the errors are those associated with a variation of m_b by ∓ 0.25 GeV. The NLO calculations predict a cross section which is about a factor of 2 below the measurements. The ZEUS collaboration published a measurement of $b\bar{b}$ production [51] for the region $p_t > 5$ GeV and $|\eta_b| < 2$:

$$\begin{aligned}\sigma(ep \to e' b\bar{b} X) &= 1.6 \pm 0.4(stat.)^{+0.3}_{-0.5}(syst.)^{+0.2}_{-0.4}(ext.) \\ &= 1.6^{+0.54}_{-0.75} \text{ nb}\end{aligned}$$

where we have added all errors quadratically in the last expression. This can be compared with the prediction from CASCADE:

$$\sigma(ep \to e' b\bar{b} X) = 0.88 \pm 0.08 \text{ nb}.$$

Again we have used $m_b = 4.75 \mp 0.25$ GeV. The predicted cross section is still within the total error of the measurement. The NLO prediction as given in [51] is $\sigma = 0.64^{+0.15}_{-0.1}$ nb, where the errors are those associated with a variation of $m_b = 4.75$ GeV by ∓ 0.25 GeV and of the factorisation and renormalisation scales by a factor of 1/2 and 2.

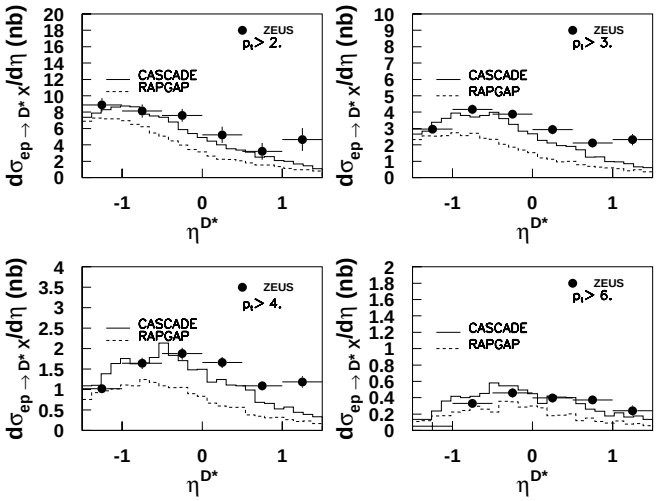

Fig. 8. The differential cross section of D^* photo-production [49] $d\sigma/d\eta^{D^*}$ for different regions of $p_t^{D^*}$. The solid line shows the prediction from CASCADE and the dashed line is the prediction from RAPGAP

6 Conclusion

We have shown that a backward evolution approach using the CCFM evolution equation is possible, and that it works, producing the same results as the forward evolution used to solve the CCFM equation. The advantage of backward evolution is the easy implementation into a full hadron-level Monte Carlo program CASCADE, which is compared to recent measurements of small x hadronic final state properties at HERA. We have found that all small x signatures can be reasonably well described within one consistent approach. By performing only a fit to the structure function $F_2(x, Q^2)$ we obtain simultaneously a good description of a variety of processes which could not be described within DGLAP: the forward-jet cross section, the high p_t particle spectra, charm production and a reasonable agreement with the measured $b\bar{b}$ cross section. This shows that the CCFM evolution equation is indeed a good starting point for a consistent description of small x phenomena.

Acknowledgements. We are very grateful to B. Webber for providing us with the SMALLX code, which was the basis of the studies presented here. We are also grateful to B. Andersson, G. Gustafson, L. Jönsson, H. Kharraziha and L. Lönnblad for all their criticism and useful ideas on CCFM and the backward evolution, to M. Ciafaloni and S. Catani for comments on the manuscript. One of us (H.J.) would like to thank A.D. Martin

and J. Kwiecinski for their explanation of the modified non-Sudakov form factor and the DESY directorate for hospitality and support.

References

1. V. Gribov, L. Lipatov, Sov. J. Nucl. Phys. **15** (1972) 438 and 675
2. L. Lipatov, Sov. J. Nucl. Phys. **20** (1975) 94
3. G. Altarelli, G. Parisi, Nucl. Phys. **B 126** (1977) 298
4. Y. Dokshitser, Sov. Phys. JETP **46** (1977) 641
5. G. Ingelman, A. Edin, J. Rathsman, Comp. Phys. Comm. **101** (1997) 108
6. T. Sjöstrand, Comp. Phys. Comm. **82** (1994) 74
7. G. Marchesini et al., Comp. Phys. Comm. **76** (1992) 465, hep-ph/9912396
8. B. Webber, Herwig 5.4, in Proc. of the Workshop on Physics at HERA Vol. 3, 1354, edited by W. Buchmüller, G. Ingelman (1991)
9. H. Jung, The RAPGAP Monte Carlo for Deep Inelastic Scattering, version 2.08, Lund University, 1999, `http://www-h1.desy.de/~jung/rapgap.html`
10. M. Ciafaloni, Nucl. Phys. **B 296** (1988) 49
11. S. Catani, F. Fiorani, G. Marchesini, Phys. Lett. **B 234** (1990) 339
12. S. Catani, F. Fiorani, G. Marchesini, Nucl. Phys. **B 336** (1990) 18
13. G. Marchesini, Nucl. Phys. **B 445** (1995) 49
14. T. Sjöstrand, Phys. Lett. **B 157** (1985) 321
15. M. Bengtsson, T. Sjöstrand, M. van Zijl, Z. Phys. **C 32** (1986) 67
16. G. Marchesini, B. Webber, Nucl. Phys. **B 310** (1988) 461
17. G. Marchesini, B. Webber, Nucl. Phys. **B 349** (1991) 617
18. G. Marchesini, B. Webber, Nucl. Phys. **B 386** (1992) 215
19. E. Kuraev, L. Lipatov, V. Fadin, Sov. Phys. JETP **44** (1976) 443
20. E. Kuraev, L. Lipatov, V. Fadin, Sov. Phys. JETP **45** (1977) 199
21. Y. Balitskii, L. Lipatov, Sov. J. Nucl. Phys. **28** (1978) 822
22. B. Andersson, G. Gustafson, J. Samuelsson, Nucl. Phys. **B 467** (1996) 443
23. B. Andersson, G. Gustafson, H. Kharraziha, J. Samuelsson, Z. Phys. **C 71** (1996) 613
24. G. Gustafson, H. Kharraziha, L. Lönnblad, The LCD Event Generator, in Proc. of the Workshop on Future Physics at HERA, edited by A. De Roeck, G. Ingelman, R. Klanner (1996), p. 620
25. H. Kharraziha, L. Lönnblad, JHEP **03** (1998) 006
26. J. R. Forshaw, A. Sabio Vera, Phys. Lett. **B440** (1998) 141
27. B. R. Webber, Phys. Lett. **B444** (1998) 81
28. G. P. Salam, JHEP **03** (1999) 009
29. C. R. Schmidt, Phys. Rev. Lett. **78** (1997) 4531
30. L. H. Orr, W. J. Stirling, Phys. Rev. **D56** (1997) 5875
31. L. H. Orr, W. J. Stirling, Phys. Lett. **B429** (1998) 135
32. G. Bottazzi, G. Marchesini, G. Salam, M. Scorletti, JHEP **12** (1998) 011, hep-ph/9810546
33. V. S. Fadin, L. N. Lipatov, Phys. Lett. **B429** (1998) 127
34. M. Ciafaloni, G. Camici, Phys. Lett. **B430** (1998) 349
35. G. Bottazzi, G. Marchesini, G. Salam, M. Scorletti, unpublished.
36. J. Kwiecinski, A. Martin, P. Sutton, Phys. Rev. **D 52** (1995) 1445
37. B. Andersson, G. Gustafson, H. Kharraziha, L. Lönnblad, private communication.
38. H. Jung, CCFM prediction for F_2 and forward jets at HERA, in Proceedings of Workshop on Deep Inelastic Scattering and QCD (DIS 99) (DESY, Zeuthen, 1999), hep-ph/9905554
39. H. Jung, CCFM prediction on forward jets and F_2: parton level predictions and a new hadron level Monte Carlo generator CASCADE, in Proceedings of the Workshop on Monte Carlo generators for HERA physics, edited by A. Doyle, G. Grindhammer, G. Ingelman, H. Jung (DESY, Hamburg, 1999), hep-ph/9908497
40. S. Catani, M. Ciafaloni, F. Hautmann, Nucl. Phys. **B 366** (1991) 135
41. T. Sjöstrand, Comp. Phys. Comm. **82** (1994) 74
42. H1 Collaboration, S. Aid et al., Nucl. Phys. **B 470** (1996) 3
43. H1 Collaboration, C. Adloff et al., Nucl. Phys. **B 538** (1999) 3
44. ZEUS Collaboration; J. Breitweg et al., Eur. Phys. J. **C 6** (1999) 239
45. ZEUS Collaboration; J. Breitweg et al., Phys. Lett. **B 474** (1999) 223
46. M. Kuhlen, Phys. Lett. **B 382** (1996) 441, hep-ph/9606246
47. M. Kuhlen, High p_t particles in the forward region at HERA, in Proc. of the Workshop on Future Physics at HERA, edited by A. De Roeck, G. Ingelman, R. Klanner (DESY, Hamburg, 1996), p. 606, hep-ex/9610004
48. H1 Collaboration, C. Adloff et al., Nucl. Phys. **B 485** (1997) 3
49. ZEUS Collaboration; J. Breitweg et al., Eur. Phys. J. **C 6** (1999) 67
50. H1 Collaboration; C. Adloff et al., Phys. Lett. **B 467** (1999) 156
51. ZEUS Collaboration; J. Breitweg et al., submitted to Eur. Phys. J. **C**, DESY 00-166 hep-ex/0011081